

## Article

# Study of a Late Bronze Age Casting Mould and Its Black Residue by 3D Imaging, pXRF, SEM-EDS, Micro-FTIR and Micro-Raman

Elin Figueiredo <sup>1,\*</sup>, Carlo Bottaini <sup>2</sup>, Catarina Miguel <sup>2</sup>, Aaron Lackinger <sup>3,4</sup>, José Mirão <sup>2</sup> and Beatriz Comendador Rey <sup>4</sup>

<sup>1</sup> Centro de Investigação de Materiais, CENIMAT/i3N, Faculdade de Ciências e Tecnologia, Universidade NOVA de Lisboa, Quinta da Torre, 2829-516 Caparica, Portugal

<sup>2</sup> Laboratório HERCULES & CityUMacau Chair in Sustainable Heritage, Universidade de Évora, Largo do Marquês de Marialva 8, 7000-809 Évora, Portugal; carlo@uevora.pt (C.B.); cpm@uevora.pt (C.M.); jmirao@uevora.pt (J.M.)

<sup>3</sup> Facultad de Filosofía y Letras, Universidad de Granada, Campus de la Cartuja sn, 18071 Granada, Spain; alackinger@ugr.es

<sup>4</sup> Grupo de Estudos de Arqueoloxía, Antigüidade e Territorio, GEAAAT, Facultade de Historia, Universidade de Vigo, Campus das Lagoas, 32004 Ourense, Spain; beacomendador@uvigo.es

\* Correspondence: esf@fct.unl.pt



**Citation:** Figueiredo, E.; Bottaini, C.; Miguel, C.; Lackinger, A.; Mirão, J.; Comendador Rey, B. Study of a Late Bronze Age Casting Mould and Its Black Residue by 3D Imaging, pXRF, SEM-EDS, Micro-FTIR and Micro-Raman. *Heritage* **2021**, *4*, 2960–2972. <https://doi.org/10.3390/heritage4040165>

Academic Editor: Francesco Paolo Romano

Received: 30 August 2021

Accepted: 24 September 2021

Published: 30 September 2021

**Publisher's Note:** MDPI stays neutral with regard to jurisdictional claims in published maps and institutional affiliations.



**Copyright:** © 2021 by the authors. Licensee MDPI, Basel, Switzerland. This article is an open access article distributed under the terms and conditions of the Creative Commons Attribution (CC BY) license (<https://creativecommons.org/licenses/by/4.0/>).

**Abstract:** In the present work, a fragment of a stone mould recently found in Galicia (NW Spain) was studied by multiple analytical techniques approach involving 3D optical imaging reconstruction to obtain data about the shape of the mould, typology of artefact produced, and distribution of a black residue at the surface of the mould and pXRF, SEM-EDS, micro-FTIR, and micro-Raman to investigate the nature of the black residue. The study shows that the mould was likely used for socketed axes with a side loop, was originally composed of two valves and one core, and that it might have been subjected to a repair during use. The black residue is distributed in the carved surface and spreads to nearby surfaces as a result of the use of the mould. The alloy cast in the mould was a ternary bronze (Cu + Sn + Pb). The analyses by SEM-EDS of black residue covering the surface did show the presence of scattered micro particles with P and Ca, and micro-Raman analysis detected the presence of a carbon black of animal source, while micro-FTIR analysis detected remains of proteins, oxalates, and hydroxyapatite. These results are amongst the very few studies made on black residues of ancient moulds and suggest that the mould was dressed with a carbon black of animal origin, such as burned bones, prior to metal casting, probably used as a coating agent to improve the casting and artefact recovery.

**Keywords:** archaeometallurgy; Late Bronze Age; casting mould; carbon black; burned bones; pXRF; SEM-EDS; micro-FTIR; micro-Raman; 3D reconstruction

## 1. Introduction

Ancient metal artefacts were often obtained in a mould. Simple moulds, such as those composed by only one piece, have been known since the Chalcolithic (4th and 3rd millennium BCE). By the Bronze Age (2nd to the first quarter of 1st millennium BCE), as a result of the development of technical skills and demand for more sophisticated shapes of artefacts, moulds became more complex.

Most of the archaeological works on metal artefact production focus on the metal artefacts themselves, with fewer studies on objects and tools that were involved in their production, such as lithic instruments used for their plastic deformation [1,2] or moulds [3–5]. As for the latter, one of the reasons might be that they are relatively rare in the archaeological record when compared to their metal cast counterparts. Nevertheless, moulds are one of the key elements along the operational chain of metal production, namely in the

shaping of an artefact, and the technologies of metal working and shaping must have run aside with mould technological improvements developments.

Moulds to produce a wide range of metal objects, e.g., axes, sickles, chisels, spear-heads, swords, bracelets, ornaments, etc., have been found across Europe [6–10] since the emergence of metallurgy. Moulds for axes are the most common ones, as also evidenced in the Iberian Peninsula [11–15]. They were produced with different materials—clay, stone, and metals—depending on the availability of raw materials and their specific properties. In the case of lithic moulds, for example, stones with softer properties and high thermal shock resistance would be best appreciated.

Stone moulds to produce axes evolved from single-piece moulds, such as a single one-sided carved stone, to bivalve moulds, such as two matching carved stones that could produce flat axes or palstaves, to later complex multi-piece moulds, such as, for example, two-valve moulds with a third piece to serve as core for hollow axes production, such as to produce socketed axes.

Recently, a large fragment of an axe stone mould was found in the islet of Guidoiro Areoso (Pontevedra, Galicia, Spain) as a direct consequence of recent coastal erosion and extreme weather events. The islet is very small (<1 km<sup>2</sup>), just some 2 km away from another islet, Guidoiro (~3 km long), and just some 5 km away from the coast of Galicia. It is part of an archipelago of small islets in the Ría de Arousa, at the north-western Atlantic coast of Iberia. The small islet is very emblematic since it is very rich in archaeological vestiges, namely in funerary structures, such as cists and mounds [16]. The archaeological excavations performed up until the present revealed structures and layers pointing to occupations since the 3rd to the 1st millennium BCE. Some emblematic artefacts found during archaeological excavations include two binary alloy bronze awls considered to be amongst the earliest bronze objects from Iberia [17,18], ceramic sherds of Bell-Beaker Pan-European typology (Late Chalcolithic/Early Bronze Age), and Cogotas I typology, typical from the Mesetas (mainland central Spain) [19]. The presence of these artefacts suggests the integration of this small islet in a large network of contacts.

The mould found in Guidoiro Areoso has its carved surface altered to black, contrasting with the rest of the grey stone-coloured surface. The finding of archaeological moulds with inner black surfaces is relatively common and it is regarded as a proof of its use. The reason for this black colour is generally assumed to be the chemical reactions between the high-temperature metal and mould material: when metal is poured, the high temperature (>1000 °C) causes easy oxidation, volatilisation, and reaction with the surface material of the mould, resulting in a typical black colour [20].

The use of a dressing or parting layer on the inner surface of the moulds is sometimes proposed for archaeological examples since it could improve the casting process and artefact detachment from the mould. However, analyses of these are very scarce. Instead, studies of moulds focus mainly on the characterisation of the mould material itself [21,22]. The study of the use of any dressing or parting layer is, however, of high interest since it relates to technical skills, innovations, and knowledge transfer, of importance in the study of ancient metal artefact production.

Different studies have proposed different dressing materials based on analysis of residues on Bronze Age mould artefacts: for example, one study suggested smoky flame from burning bones based on results from energy dispersive X-ray spectrometry (EDXRF), wet chemistry, Fourier transform infrared spectroscopy (FTIR), and gas chromatography mass spectrometry (GC/MS) from the black residue in a stone axe mould from Portugal [23]; another study proposed the use of beeswax based on results from FTIR and GC/MS from a black residue in a bronze axe mould from Poland [24]; finally, more recently, a blackish residue on the inner face of a Late Bronze Age mould from Portugal has been analysed by FTIR, revealing the use of clay or charcoal [14].

Generally, carbon-based materials can be categorised into graphite, flame carbons, chars, or cokes, according to their source material and manufacturing process [25]. However, discriminating among these carbon black materials, especially in archaeological or

other cultural heritage objects, is complex, and multi-analytical approaches are required. Most frequently, studies of black carbon materials are made on ancient and historical pigments, and the use of a combination of elemental, e.g., X-ray fluorescence (XRF) and scanning electron microscopy with energy dispersive X-ray analysis (SEM-EDS), structural, e.g., X-ray diffraction (XRD), molecular, e.g., Fourier-transform infrared spectroscopy (FTIR) and Raman, and morphological analysis of particles, e.g., secondary electron (SE) and backscattered electron (BSE) imaging modes in SEM-EDS, have been shown to be needed [25,26].

In the present work, the Guidoiro Areoso mould is studied by optical imaging with 3D reconstructions to evaluate its shape and to map the areas with black residue. Portable XRF (pXRF) analysis is made over surfaces with the black residue and results compared with analysis of the stone surface for the search of elements related to the type of metal that was being poured. Detailed SEM-EDS, micro-FTIR, and micro-Raman analysis are performed on samples of the black residue to investigate its nature. The results are amongst the very few studies performed on black residues found in prehistoric moulds of Western Europe and will provide the first data of this kind for the north of the Iberian Peninsula.

## 2. Materials and Methods

### 2.1. The Mould

The stone axe mould found in Guidoiro Areoso belongs to one valve and is made of aplite, a granitic-type rock that is abundant in Galicia and North of Portugal. The valve is incomplete since it has been fractured on one side top. The carved part of the valve intended for the metal accommodation has its surface covered with a dark residue. This dark residue, which can be described as a black greasy powder that sticks to its surface, spreads out of the carved area and accumulates in a frame-like shape at the parting face of the valve (the surface that was in contact with the other valve) and also to the top surface, where it is present in a circular shape. Accumulations of this black material in sufficient quantity for easy sampling happens in corners of the engraved surface.

### 2.2. Methods

#### 2.2.1. 3D Reconstruction and Optical Imaging

A total of 102 overlapping photographs were taken of the mould from various angles with a digital camera Olympus E-420. These images were processed with Agisoft Photoscan PRO software for a 3D reconstruction by the photogrammetry method. The produced model combines the data of the shape and texture of the mould. Visualisation of the 3D model was made in the freely available software MeshLab and Fiji/ImageJ.

Detailed observations of the back residue were made with a stereo zoom optical microscope Leica M205C, with a camera Leica DFC290HD for image acquisition. The recording of the presence of black residue at different areas was made, providing details of its accumulation at corners of the engraved area. Sampling in these areas was made with the assistance of the stereomicroscope observations.

#### 2.2.2. Portable X-ray Fluorescence Spectrometry (pXRF)

Elemental analyses were made with a handheld pXRF over the surface of the mould in areas with and areas without the black residue. Analyses were made with a Bruker Tracer IV-SD equipped with a Rh target X-ray tube (12 W), a silicon drift detector with a resolution better than 150 eV (Mn-K $\alpha$ ), and a five-position computer-controlled filter changer. The spot size of the analysis is  $\sim 7$  cm<sup>2</sup>. The working conditions were 40 kV of tube voltage, 14  $\mu$ A of current intensity, and 60 s of acquisition time for each measurement. Analyses were made with a Ti/Al filter. The software ARTAX 7.4 was used for qualitative spectra analysis.

### 2.2.3. Scanning Electron Microscopy Coupled with Energy-Dispersive X-ray Spectroscopy (SEM-EDS)

Elemental microanalysis and microstructure examination were performed by a variable pressure SEM-EDS on samples of black residue.

The equipment used was a HITACHI S-3700N with a secondary electrons detector (SE), backscattered electrons detector (BSE), and an energy dispersive spectrometer (EDS). The EDS is an XFlash 5010 Silicon Drift Detector (SDD) with a resolution of 129 eV (Mn-K $\alpha$ ), from Bruker.

Analyses were made without surface preparation, i.e., without gold or carbon coating. Experimental conditions involved variable acceleration voltages 5–20 kV depending on the average atomic number of materials analysed, 100–120  $\mu$ A emission current, and 10–12 mm working distance. The chamber pressure was 30 Pa. Standardless semi-quantitative analyses were made using the ZAF correction procedure.

### 2.2.4. Micro-Fourier Transform Infrared Spectroscopy (Micro-FTIR)

Micro-FTIR analysis was carried out using a Bruker Hyperion 3000 spectrophotometer with a Mercury Cadmium Telluride detector cooled by liquid nitrogen and a 15 $\times$  objective lens. The spectra were collected in the transmission mode, in 50–100  $\mu$ m areas, in the 4000–600  $\text{cm}^{-1}$  region with a resolution setting of 4  $\text{cm}^{-1}$  and 64 scans, using an S.T. Japan diamond anvil compression cell. The spectra discussed in the present work are shown as acquired, without corrections or any further manipulations.

### 2.2.5. Micro-Raman Spectroscopy

Micro-Raman analysis was performed using a HORIBA XPlora spectrometer equipped with a HeNe laser of 11 mW power operating at 638 nm, coupled to an Olympus microscope. Raman spectra were acquired as an extended range in the 100–2000  $\text{cm}^{-1}$  region. The laser spot was focused with a 50 $\times$  Olympus objective lens, with a laser power at the surface of the sample of 1.1 mW (10 s of acquisition time, 10 cycles of accumulation) and an 1800 gr/mm diffraction grating. To improve the readability of the spectrum, a baseline smooth correction (second-order polynomial, 13-point window width, five-point window length) was followed.

## 3. Results and Discussion

### 3.1. Shape of the Mould and Black Residue Distribution

The 3D reconstruction of the mould (Supplementary Materials Figure S1) allows the observation and enhancement of the shape and texture of the surface. In Figure 1 on the left a photograph of the mould (front view) is shown, and in the centre and at the right are projections of the mould in two different positions extracted from the 3D reconstruction. One of the images is shown with texture uploaded to evidence the distribution of the dark residue. The other two images (in green) demonstrate the shape of the mould and surface morphology. It is visible that at the top of the mould, grooves were made, and that at the broken surface, there are four holes, one of these intersecting another (the position of the holes are highlighted by the arrows).

The images show that the black residue is distributed in the cavity and around it in the shape of a rim (a bit is missing due to loss of mould material at the corner of the parting face) and on the top of the mould in a round-shape. The distribution of the dark residue out of the cavity can be explained due to the escape of gases and metal flashing during pouring. In Figure 2, the accumulation of the black residue can be observed under higher magnifications, at the parting face, and in a corner of the cavity, where sampling was performed.

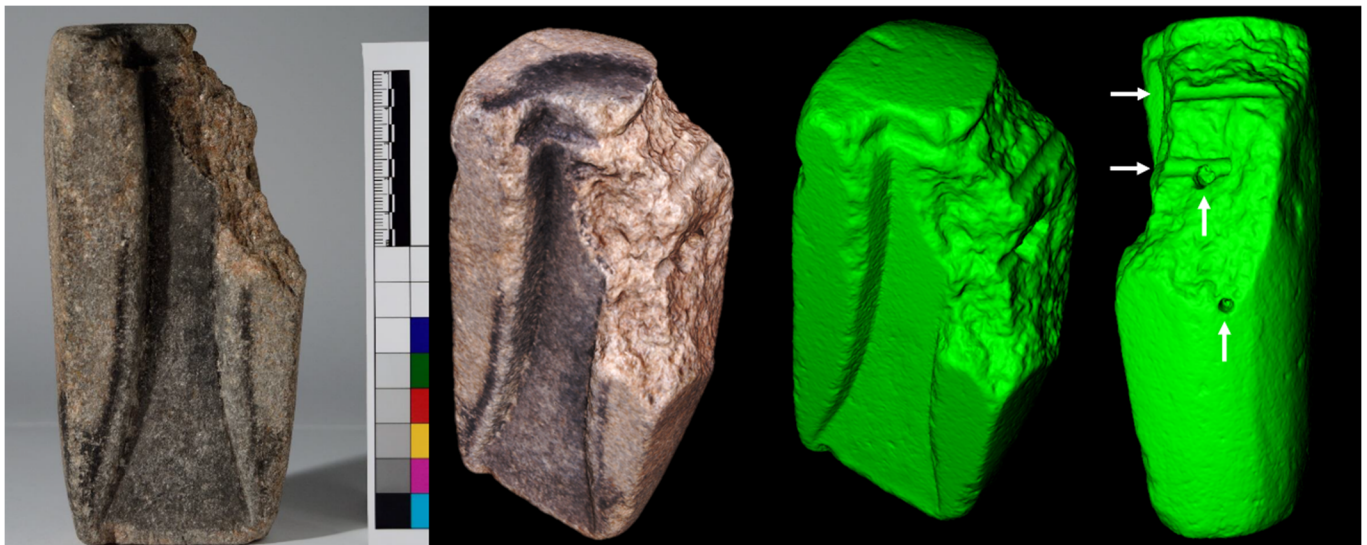


**Figure 1.** At (left) a front view photograph of the studied mould. At (centre, right) (over a black background) projections of the 3D reconstruction of the mould: in the first image, the texture of the mould has been added, demonstrating the distribution of the black residue over different surfaces; in the two green images, the shape of the mould and morphology of surfaces can be better appreciated, demonstrating areas with material loss and the four holes (positions highlighted with white arrows).

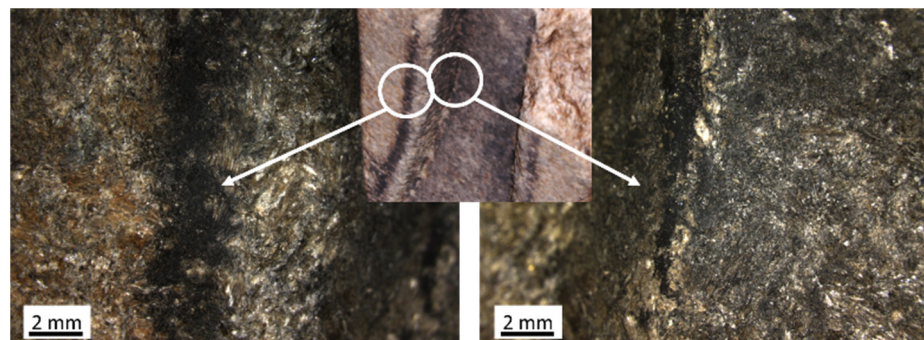


**Figure 2.** Detailed images by stereo microscope showing the black residue on the inner surface of the mould: (at left) accumulation in a rim shape at the parting face and (at right) accumulation in the corner of the cavity.

The mould was originally made of two valves. A simulation of the cross-section of two valves (Figure 3) shows that the axe produced had a near quadrangular cross-section. This shape is typical for a socketed axe, which is an axe with an internal hole. This hole would have served to place a wooden shaft and would have been shaped by a core placed at the top part of the mould. This core could also have formed the casting opening by incorporating channels (where the metal would flow into the mould).

Socketed axes are known in Galicia [11,27], and in the area of Pontevedra at least three axes have been found that show very similar shapes to the axe that was produced in the Guidoiro Areoso mould, namely n. 1687 from Vilaboa (Pontevedra), n. 1688 from Pontecaldelas (Pontevedra), and n. 1689 from Prov. Pontevedra described in Monteagudo [11]. In Figure 3, one of these axes is shown to scale with the mould. It is worth noting the near-perfect fit and that it appears that the axe has been severely worn out (due to use?) at the cutting edge, and that the broken part of the mould could correspond to the area of a loop.

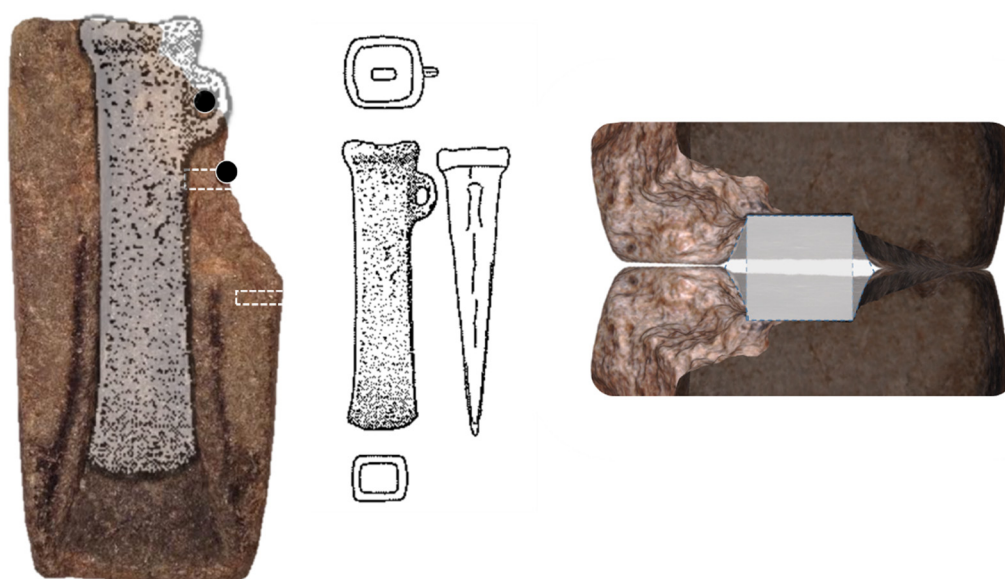


**Figure 3.** Mould from Guidoiro Areoso and its relation to socketed axe production: (at **left**) mould with a superimposed image of a representation of a socketed axe found in Vilaboa (Pontevedra, Galicia) (in same scale; the location of the holes for dowels are annotated; note that probably the axe found in Vilaboa is shortened due to use-wear); (at **middle**) representation of the socketed axe from Vilaboa (different views), redrawn from Monteagudo [11]; (at **right**) reconstruction of the cross-section of the axe that would have been produced in the Guidoiro Areoso mould.

Additionally, at least three other fragments of moulds to produce socketed axes are known in the region, one from Cuntis (Pontevedra), another from Castro de Montealegre (Moaña, Pontevedra), and another from O Neixón Pequeno (Boiro, La Coruña, Ría de Arousa). The mould from O Neixón Pequeno does also have a broken top part and also present holes (a total of two). The two holes in the O Neixón Pequeno mould are in the broken area, which in this case is at the opposite side of the loop, and reach the outer surface of the mould in diagonal in respect to the inner surface. The suggestion made here is that the holes of the Guidoiro mould, or at least some of them, were part of a repair effort, by using a binding/clustering solution of the broken piece to the rest of the mould. Broken parts could be bound together through the use of dowels (likely wooden pins) fitted in the holes. A combination, for example, of cords on the outer side would help the bond/union. The grooves at the top of the mould could serve for cords that could help to place the core piece in place but also the broken part. The direction of the grooves argues against their function being to bind the two valves together.

It is common to find grooves and/or dowels in Late Bronze Age moulds, used to fit the two valves correctly together to prevent faulty matchings. In the present case, no apparent system was found. However, it can be possible that the two holes that are perpendicular to the parting face could have served to pin the two valves together. In that case, one of the dowels could also have made the core of the loop (if existent).

The hypothesis that the mould was broken and repaired to be used can also find some support on the observation of the black residue. This residue does also spread over the border of the fracture, suggesting that the fracture already existed when casting was made.

Likely, stone moulds would have been of significant value in pre-historical times; once, they were objects that involved much time and technical skill to produce, and their use would allow “mass” production of metal objects, making them worthy of repair.

### 3.2. Analysis of the Mould by pXRF

Analyses by pXRF were made on the surface of the mould at different areas, including areas with the black residue and areas without it. Spectra from both types of areas were compared to search for the presence of elements related only to the black residue. In all the spectra, peaks corresponding to Si ( $K\alpha$ ), Ca ( $K\alpha$ ,  $K\beta$ ), Ti ( $K\alpha$ ), Cr ( $K\alpha$ ), Mn ( $K\alpha$ ), Fe ( $K\alpha$ ,

K $\beta$ ), Ni (K $\alpha$ , K $\beta$ ) and Zn (K $\alpha$ ) were present. The intensities of the peaks remained similar through all spectra. However, in the spectra taken in the areas with the black residue, peaks corresponding to Cu (K $\alpha$ , K $\beta$ ) and Pb (L $\alpha$ , L $\beta$ ) were also present. In Figure 4, a spectrum of the stone (taken at the back of the mould) with two spectra taken over the black residue, one in the middle of the cavity and the other at the top of the mould, are shown. The analyses show that the black residue incorporates elements from the metal cast (which are not present in the mould material) and can provide information about the type of metal that was being used. It has been shown in experimental castings that from those metals used in antiquity (Cu, Sn, Pb, and Zn), those that adhere easily to the surface of the mould are Pb, Zn, and Cu and to a much lesser extent Sn [20]. Thus, taking into consideration the present analysis and that socketed axes were frequently made of a ternary bronze alloy (Cu-Sn-Pb) [28,29], it seems that a ternary bronze was the type of alloy cast in the mould.

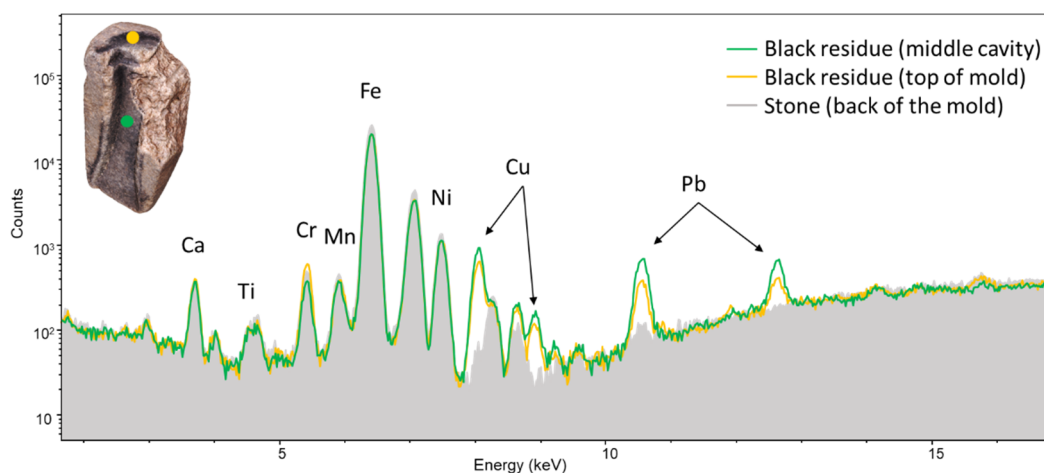


**Figure 4.** XRF spectra of the mould showing the presence of Cu and Pb related to the black residue: (solid grey) spectrum from the back of the stone; (outline yellow) spectrum from the top of the mould over the black residue; (outline green) spectrum from the carved area with the black residue.

### 3.3. Analysis of the Black Residue by SEM-EDS

Elemental and morphological analysis by SEM-EDS to the black residue particles sampled from the mould showed that the residue is heterogeneous at the microscale level. BSE images show areas with a higher average atomic number than others, and elemental EDS point analyses show that these areas have a strong presence of Sn (L lines) (Figure 5). The other elements related to the metal are also detected in spot analysis over different areas, namely the Cu (K and L lines) and Pb (L and M lines).

Besides the elements related to metal (Cu, Sn, and Pb), other elements such as Mg, Al, Si, P, S, Cl, K, Ca, and Fe were detected. The presence of K is found in some plate-like structures, and its presence is typical for vegetable charcoal [25]. Of interest was the association of P and Ca in scattered particles, as shown in Figure 6. The presence of particles with this association of elements suggests apatite mineral. Apatite can be of geological or biological origin, e.g., bones are ~70% carbonated hydroxyapatite. Topographic images by SE show that these particles have fragmented surfaces, with a hexagonal-like plate pattern, a morphology found in hydroxyapatite from burned bones and teeth [30,31]. Additionally, EDS spot analysis of these particles shows carbon contents in the range of 20–50%, which with the presence of phosphorous suggests a carbon black of bone origin [25].

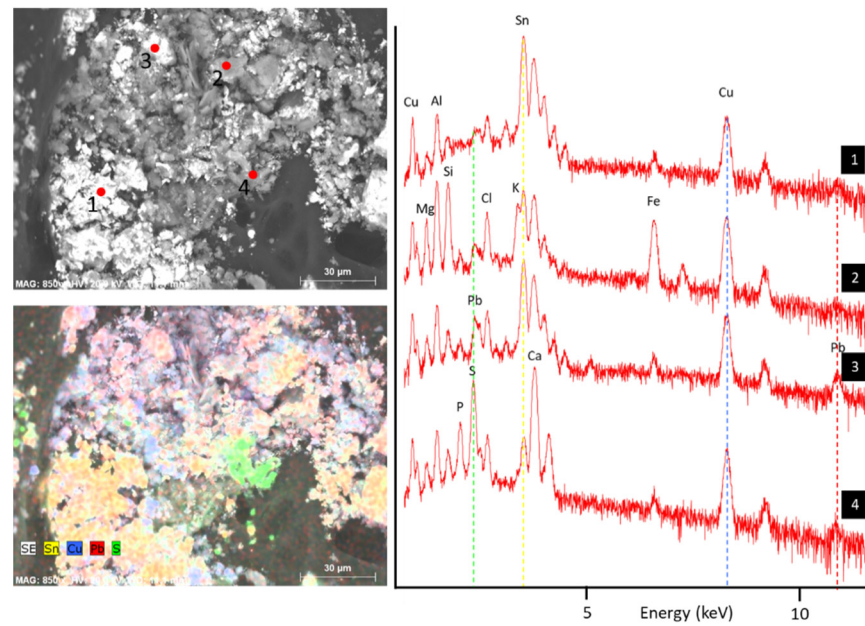


**Figure 5.** SEM-EDS analysis of the black residue of the mould: (at **top left**) BSE atomic contrast image depicting the locations of EDS spot analysis; (at **bottom left**) SE topographic contrast image with elemental mapping for Sn, Cu, Pb, and S; (at **right**) spectra of the four EDS spot analysis with the characteristic lines (Sn, Cu, Pb, S) depicted that were used for the elemental mapping: (1) spectrum most Sn-rich; (2) spectrum most Fe-rich; (3) spectrum Pb-rich; (4) spectrum most S-rich.

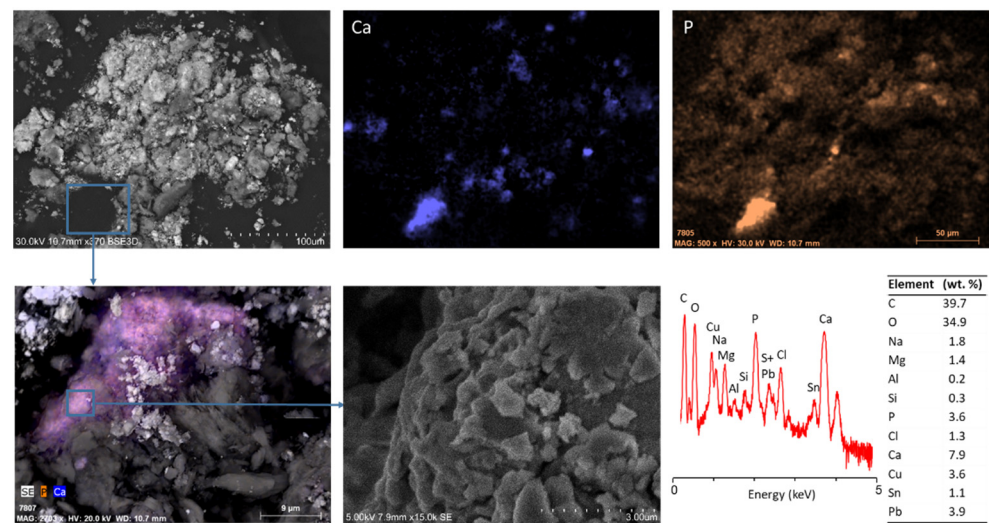


**Figure 6.** SEM-EDS detailed analysis of particles rich in P and Ca (hydroxyapatite) in the dark residue: (top) BSE image of an agglomerate of particles and maps of Ca and P (note that Ca mapping was obtained by subtracting Sn influence—due to peak overlap); (bottom left) SE image with mapping of P and Ca superimposed on one particle; (bottom centre) detailed SE image of the surface of one particle rich in P and Ca (hydroxyapatite); (bottom right) spectra of EDS spot analysis to a particle rich in P and Ca and semi-quantitative results.

### 3.4. Analysis of the Black Residue by Micro-FTIR and Micro-Raman

Micro-FTIR analysis of the black residue from the mould allowed the identification of absorption bands related to organic compounds, namely the bands at 2961, 2929, 2876, and 2855  $\text{cm}^{-1}$  attributed to the stretching vibrations of the methyl and methylene groups. Bands that are considered characteristic of protein content are observed at 1644 and 1557  $\text{cm}^{-1}$ , the Amide I and Amide II stretches (Figure 7) [32]. The low-resolution of

the Amide I and Amide II absorption bands might be due to the presence of an absorption band at  $1610\text{ cm}^{-1}$  assigned to the  $\nu(\text{C}=\text{O})$  of oxalates [30]. Previous works regarding the influence of heat on bone diagenesis suggest that at temperatures between  $400\text{--}550\text{ }^{\circ}\text{C}$ , there is a decomposition of both lipids and proteins present in the bone's composition [33]. Considering that the molten bronze exposed the internal surface of the mould to temperatures  $>900\text{ }^{\circ}\text{C}$ , it is expected a decomposition of the organic compounds that could have been present in the original formulation of this black residue. In this sense, the organic fingerprints present in the FTIR spectrum (Figure 7) are likely related to the presence of a contamination (e.g., by microorganisms since the mould was buried during more than two millennia) and not related to an original remain of an organic compound. Finally, the bands at  $1111$  and  $1031\text{ cm}^{-1}$  might be related to the presence of  $(\text{PO}_4^{3-})$  groups of hydroxyapatite ( $\text{Ca}_5(\text{OH})(\text{PO}_4)_3$ ). The bands at  $1454$ ,  $1404$ , and  $790\text{ cm}^{-1}$  can be related to the stretching vibrations of calcium carbonate of carbonated hydroxyapatite, expected for bone samples (Figure 7) [25].

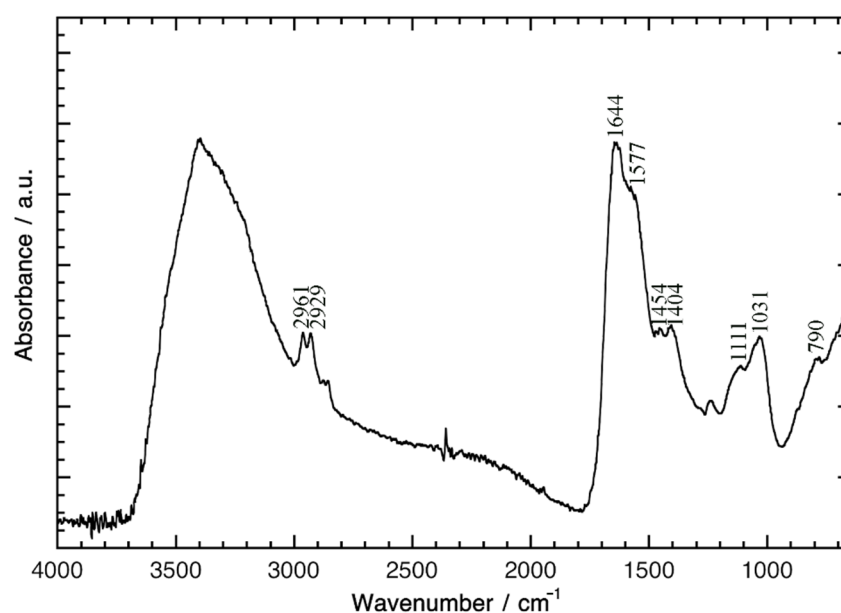
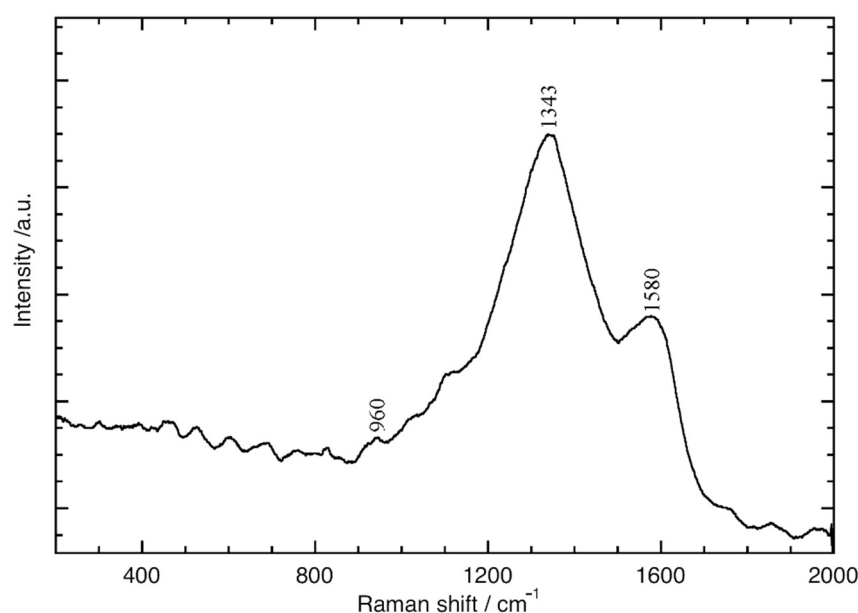


Figure 7. Micro-FTIR spectra of a sample of the black residue.

Micro-Raman analysis allowed the identification of a carbon-black based material. The higher intensity of the Raman D band at  $1343\text{ cm}^{-1}$  related to the disorder degree of graphite structure, when compared with the G band at  $1583\text{ cm}^{-1}$  (less intense), which is related to the graphitisation degree of the structure, suggests the presence of a carbon-disordered black residue [26,34] (Figure 8). A word should be expressed for the very low-intensity Raman band at ca.  $960\text{ cm}^{-1}$  (Figure 8) related to the stretching of the phosphate groups. Typically, this very low-intensity Raman band is not always easily detected, and its identification is highly dependent on the measurement conditions [34]. For this, the Raman fingerprints for the presence of a carbon-disordered black together with the results of SEM-EDS analysis, where it was possible to identify the presence of particles of phosphorus and calcium, and of micro-FTIR, where it was identified absorption bands related with the presence of phosphate and hydroxyapatite, support the attribution of this low Raman fingerprint at  $960\text{ cm}^{-1}$  and, together with SEM-EDS and micro-FTIR, suggest that the mould was intentionally dressed with a carbon black that had bones in its source material.



**Figure 8.** Micro-Raman spectra of a sample of the black residue.

### 3.5. Conclusions

The present study showed that the mould from Guidoiro Areoso was used to produce socketed axes, likely with a loop, a typology that was at use in the northwest of the Iberian Peninsula during the Late Bronze Age/Early Iron Age. It is concluded that the metal used to produce the axe was a ternary bronze (Cu-Sn-Pb), provided that the elements Cu and Pb were detected by pXRF in the black residue that covers the cavity and part of surrounding surfaces, and Cu, Pb and Sn were detected by SEM-EDS in samples taken from the black residue. This type of alloy was in regular use during the Late Bronze Age/Early Iron Age in Western Europe and is distinct from the binary alloy of the awls found previously in the islet from an earlier period. The presence of this mould can provide evidence for metallurgical activity on the islet at this later period.

The mould seems to have suffered a fracture/break that was repaired with the aid of holes and dowels, a technique that seems to also have been employed in another mould from the region and from the same period.

The study of the black residue showed that it is an aggregate of particles that can be heterogeneous in their composition. The aggregate suffers from widespread contamination, with Cu and Pb being preferentially concentrated in some particles. Scattered particles with relatively high amounts of P and Ca were found that relate to the presence of apatite. Micro-Raman analysis shows a spectrum typical of a carbon black, with the D band ( $1343\text{ cm}^{-1}$ ) > G band ( $1583\text{ cm}^{-1}$ ) together with a very-low signal at  $960\text{ cm}^{-1}$  of phosphate groups, suggesting an animal source. The micro-FTIR analysis show a spectra with bands related to proteins and to the presence of phosphate groups, namely hydroxyapatite.

The complementary results suggest that (at least) part of the black residue is a product of the carbonisation of bones.

The use of a dressing with carbon black could beneficiate the casting process as it would serve to (1) smooth the carved surface, providing a higher quality surface finishing of the cast; (2) facilitate the detachment of metal and mould parts by functioning as a thin parting layer; and (3) provide a barrier to moisture, thus being of great utility in regularly used moulds (thermal shock and water vapour pressure is a cause of a fracture and severe damage of moulds that have not been adequately dried and/or pre-heated prior to casting).

The reason for the use of burned bones is, however, not clear. Possibly, bones would produce a material with higher adhesive properties than just carbonised wood (i.e., more sticky, due to decomposition of collagen/proteins and bone grease). Future analysis of black residues from other European moulds could provide further information on dressing

materials, such as if the use of carbonised bones was of widespread and in regular use, and provide further knowledge of ancient casting technologies.

**Supplementary Materials:** The following are available online at <https://www.mdpi.com/article/10.3390/heritage4040165/s1>, Figure S1: 3D interactive reconstruction of the mould.

**Author Contributions:** E.F. coordinated the study, performed the SEM-EDS and pXRF data analysis, produced the 3D projections and was a major contributor in writing the manuscript and at final revision. C.B. performed the 3D reconstruction, provided with archaeological background, and the manuscript revision. C.M. performed micro-FTIR and micro-Raman analysis and data interpretation. J.M. performed pXRF analysis and final revision. A.L. produced the supplementary interactive 3D visualisation and with B.C.R. provided archaeological background and archaeometallurgical contexts. All authors have read and agreed to the published version of the manuscript.

**Funding:** This work was funded by FEDER funds through the COMPETE 2020 Programme (European Regional Development Fund through the regional program of Lisbon and Alentejo) and National Funds through FCT (Portuguese Foundation for Science and Technology) under the Project IberianTin (PTDC/HAR-ARQ/32290/2017) and under the project UIDB/50025/2020-2023 to CENIMAT/i3N and the project number, reference UIDB/04449/2020 and UIDP/04449/2020 to HERCULES Laboratory, and DL57/2016/CP1372/CT0012 (Norma Transitória) (C.M.). C.B., C.M. and J.M. also acknowledge the City University of Macau.

**Institutional Review Board Statement:** Not applicable.

**Informed Consent Statement:** Not applicable.

**Data Availability Statement:** Data generated and analysed during this study are available from the corresponding author upon reasonable request.

**Acknowledgments:** Authors acknowledge Sónia Costa for the front view photograph of the mould. The Grupo Pandulleiros and Juan Carlos Collazo are specially acknowledged for access to the mould, which was recovered by Tomás Álvarez.

**Conflicts of Interest:** The authors declare that they have no competing interests.

## Abbreviations

3D	three dimensions
BCE	before common era
BSE	backscattered electron (imaging mode in SEM-EDS)
EDXRF	energy dispersive X-ray spectrometry
GC/MS	gas chromatography mass spectrometry
Micro-FTIR	micro-Fourier transform infrared spectroscopy
pXRF	portable X-ray spectrometry
SDD	silicon drift detector
SE	secondary electron (imaging mode in SEM-EDS)
SEM-EDS	variable pressure scanning electron microscopy
XRD	X-ray diffraction
ZAF	atomic-number effect, absorption effect, and fluorescence excitation effect (quantitative correction method)

## References

- Cardoso, J.L.; Boutille, L.; Brandherm, D. Instrumentos líticos para a deformação plástica de metais do povoado calcolítico de Outeiro Redondo (Sesimbra). *Estud. Arqueol. Oeiras* **2018**, *24*, 291–306.
- Delgado-Raack, S.; Risch, R. Lithic perspectives on metallurgy: An example from Copper and Bronze Age south-east Iberia. In *“Prehistoric Technology” 40 Years Later. Functional Studies and the Russian Legacy*; BAR International Series 1783; Longo, L., Skakun, N., Eds.; Archaeopress: Oxford, UK, 2008; pp. 235–252.
- Barbieri, M.; Cavazzuti, C. Stone Moulds from Terramare (Northern Italy): Analytical Approach and Experimental Reproduction. *EXARC Online J.* 2014. Available online: <https://exarc.net/ark:/88735/10145> (accessed on 4 November 2018).

4. Boutoille, L. Les dépôts de moules lithiques de fondeur de l'Âge du Bronze découverts en France. In *Du matériel au spirituel: Réalités archéologiques et historiques des «dépôts» de la Préhistoire à nos jours*; Bonnardin, S., Hamon, C., Lauwers, M., Quilliec, B., Eds.; Éditions APDCA: Antibes, France, 2009; pp. 379–386.
5. Fraile Vicente, A. Moldes de fundición de la Edad del Bronce en la Península Ibérica: Ensayo Tipológico y Cartográfico. Master's Thesis, Universidad de Valladolid, Valladolid, Spain, 2007.
6. Ó Faoláin, S. *Bronze Artefacts Production in Late Bronze Age Ireland. A Survey*; British Series 382; BAR: Oxford, UK, 2004.
7. Armbruster, B.; Jockenhövel, A.; Kapuran, A.; Ramadanski, R. The moulds from Velebit and European Bronze Age metal anvils. *Starinar* **2019**, *69*, 139–182. [[CrossRef](#)]
8. Webley, L.; Adams, S. Material genealogies: Bronze moulds and their castings in Later Bronze Age Britain. *Proc. Prehist. Soc.* **2016**, *82*, 323–340. [[CrossRef](#)]
9. Vilaça, R.; Almeida, S.; Bottaini, C.; Marques, J.N.; Montero-Ruiz, I. Metalurgia do Castro do Cabeço da Argemela (Fundão): Formas, conteúdos, produções e contextos. In *Povoamento e exploração dos recursos minérios na Europa Atlântica Ocidental*; Martins, C.M.B., Bettencourt, A.M.S., Martins, J.I.F.P., Carvalho, J., Eds.; CITCEM: Braga, Portugal, 2011; pp. 427–452.
10. Iaia, C. Smith and smithing in Bronze Age “Terramare”. In *Archaeology and Craft, Proceedings of the VI OpenArch-Conference in Albersdorf, Germany, 23–27 September 2013*; Kelm, R., Ed.; Husum Druck: Husum, Germany, 2015; pp. 78–93.
11. Monteagudo, L. *Die Beile auf der Iberischen Halbinsel*; Prähistorische Bronzefunde Abteilung IX, 6. Band; C.H. Beck: München, Germany, 1977.
12. Teixeira, C. Molde de fundição para machados de bronze de duplo anel. *Trab. Soc. Port. Antropol. E Etnol.* **1939**, *9*, 126–130.
13. García-Vuelta, O.; Cuesta-Gómez, F.; Galán Domingo, E.; Montero Ruiz, I. Los moldes de fundición de bronce para hachas de talón de La Macolla (Linares de Riofrío, Salamanca). Nuevos datos sobre viejos hallazgos. *Zephyrus* **2014**, *74*, 117–141. [[CrossRef](#)]
14. Senna-Martinez, J.C.; Valério, P.; Casimiro, M.H.; Ferreira, L.M.; Araújo, M.F.; Peixoto, H. Foundry in the Late Bronze Age Baiões/Santa Luzia Cultural Group: Some reflections starting from a new metallic mould for unifacial palstaves. *Ophiussa* **2018**, *4*, 51–70. [[CrossRef](#)]
15. Harrison, R. A Late Bronze Age mould from Los Oscos (prov. Oviedo). *Madr. Mitt.* **1980**, *21*, 131–139.
16. Rey, J.M.; Vilaseco, X.I. Guidoiro Areoso. Megalithic cemetery and Prehistoric settlement in the Ría de Arousa (Galicia, NW Spain). In *Environmental Changes and Human Interaction Along the Western Atlantic Edge*; Campar Almeida, A., Bettencourt, A.M.S., Moura, D., Monteiro-Rodrigues, S., Caetano Alves, M.I., Eds.; Associação Portuguesa para o Estudo do Quaternário: Coimbra, Portugal, 2012; pp. 243–258.
17. Comendador Rey, B.; Reborelda-Morillo, S.; Kockelmann, W.; Macdonald, M.; Bell, T.; Pantos, M. Early Bronze Technology at the Land's End, North Western Iberia. In *Science and Technology in Homeric Epics*; Paipetis, S.A., Ed.; Springer: New York, NY, USA, 2008; pp. 113–131.
18. Comendador, B.; Bettencourt, A.M.S. Nuevos datos sobre la primera metalurgia del Bronce en el Noroeste de la Península Ibérica: La contribución de Bouça da Cova da Moura (Ardegães, Maia, Portugal). *Estud. Quaternário* **2011**, *7*, 19–31.
19. López-Romero, E.; Güimil-Fariña, A.; Mañana Borrás, P.; Otero Vilariño, C.; Prieto Martínez, M.P.; Rey García, J.M.; Vilaseco Vázquez, X.I. Later prehistoric settlements and monuments on the islet of Guidoiro Areoso (Ría de Arousa, Pontevedra): Research on present-day littoral dynamics on the Atlantic coast. *Trab. Prehist.* **2015**, *72*, 353–371. [[CrossRef](#)]
20. Kearns, T.; Martínón-Torres, M.; Rehren, T. Metal do mould: Alloy identification in experimental casting moulds using XRF. *Hist Metall.* **2010**, *44*, 48–58.
21. Lee, C.H.; Kim, J.; Lee, M.S. Petrography and provenance interpretation of the stone moulds from bronze daggers from the Galdon Prehistoric site, Republic of Korea. *Archaeometry* **2010**, *52*, 31–44. [[CrossRef](#)]
22. Liu, S.; Wang, K.; Cai, Q.; Chen, J. Microscopic study of Chinese bronze casting moulds from the Eastern Zhou period. *J. Archaeol. Sci.* **2013**, *40*, 2402–2414. [[CrossRef](#)]
23. Soares, A.M.M.; Valério, P.; Frade, J.C.; Oliveira, M.J.; Patoilo, D.; Ribeiro, I.; Arez, L.; Santos, F.J.C.; Araújo, M.F. A Late Bronze Age stone mould for flat axes from Casarão da Mesquita 3 (São Manços, Évora, Portugal). In *Proceedings of the 2nd International Conference Archaeometallurgy in Europe, Aquileia, Italy, 17–21 June 2007*; Craddock, P.T., Giunliia-Mair, A., Hauptman, A., Eds.; Associazione Italiana di Metallurgia: Milan, Italy, 2007; pp. 145–157.
24. Baron, J.; Miazga, B.; Ntaflos, T.; Puziewicz, J.; Szummy, A. Beeswax remnants, phase and major element chemical composition of the bronze age mould from Gaj Olawsky (SW Poland). *Archaeol. Anthropol. Sci.* **2016**, *8*, 187–196. [[CrossRef](#)]
25. Tomasini, E.; Siracusano, G.; Maier, M.S. Spectroscopic, morphological and chemical characterization of historic pigments based on carbon. Paths for the identification of an artistic pigment. *Microchem J.* **2012**, *102*, 28–37. [[CrossRef](#)]
26. Tomasini, E.P.; Gómez, B.; Halac, E.B.; Reinoso, M.; Di Liscia, E.J.; Sirusano, G.; Maier, M.S. Identification of carbon-based black pigments in four South American polychrome wooden sculptures by Raman microscopy. *Heritage Sci.* **2015**, *3*, 1–8. [[CrossRef](#)]
27. Hardaker, R. Las hachas de cubo en la Península Ibérica. *Cad. De Prehist. Y Arqueol. Castellon.* **1976**, *3*, 151–171.
28. Bottaini, C.; Giardino, C.; Paternoster, G. Estudo de um conjunto de machados metálicos no Norte de Portugal. *Estud. Arqueol. Oeiras* **2012**, *19*, 19–34.
29. Bottaini, C. Depósitos Metálicos no Bronze Final (Sécs. XIII-VII a.C.) Do Centro e Norte de Portugal. Aspectos Sociais e Arqueometalúrgicos. Ph.D. Thesis, University of Coimbra, Coimbra, Portugal, 2013.
30. Shipman, P.; Foster, G.; Schoeninger, M. Burnt bones and teeth: And experimental study of color, morphology, crystal structure and shrinkage. *J. Archaeol. Sci.* **1984**, *11*, 307–325. [[CrossRef](#)]

31. Nicholson, R.A. A morphological investigation of burnt animal bone and an evaluation of its utility in archaeology. *J. Archaeol. Sci.* **1993**, *20*, 411–428. [[CrossRef](#)]
32. Miguel, C.; Clarke, M.; Melo, M.J.; Lopes, J.A. Combining infrared spectroscopy with chemometric analysis for the characterization of proteinaceous binders in medieval paints. *Chemometr. Intell. Lab. Syst.* **2012**, *119*, 32–38. [[CrossRef](#)]
33. Marques, M.P.M.; Mamede, A.P.; Vassalo, A.R.; Makhoul, C.; Cunha, E.; Gonçalves, D.; Parker, S.F.; Batista de Carvalho, L.A.E. Heat-induced bone diagenesis probed by vibrational spectroscopy. *Sci. Rep.* **2018**, *8*, 15935. [[CrossRef](#)]
34. Coccato, A.; Jehlicka, J.; Moens, L.; Vandenaabeele, P. Raman spectroscopy for the investigation of carbon-based black pigments. *J. Raman. Spectrosc.* **2015**, *46*, 1003–1015. [[CrossRef](#)]